Thin Solid Films 536 (2013) 63–67

Contents lists available at SciVerse ScienceDirect

Thin Solid Films

journal homepage: www.elsevier.com/locate/tsf

CeO_x/Al_2O_3 thin films on stainless steel substrate — Dynamical X-ray photoelectron spectroscopy investigations

Ivalina Avramova [a,b,*], Sefik Suzer [a], Desislava Guergova [c], Dimitar Stoychev [c], Plamen Stefanov [b]

[a] Department of Chemistry, Bilkent University, Ankara 06800, Turkey
[b] Institute of General and Inorganic Chemistry, Bulgarian Academy of Sciences, Sofia 1113, Bulgaria
[c] Institute of Physical Chemistry, Bulgarian Academy of Sciences, Sofia 1113, Bulgaria

ARTICLE INFO

Article history:
Received 7 February 2012
Received in revised form 21 February 2013
Accepted 22 March 2013
Available online 2 April 2013

Keywords:
Mixed oxide surfaces
Electrochemical deposition
Dynamical X-ray photoelectron spectroscopy

ABSTRACT

The CeO_x/Al_2O_3 thin films on stainless steel with different ceria loading were subjected to a.c. (square wave) pulses at various frequencies in the range 10^{-3} to 100 kHz while recording X-ray photoelectron spectra. The resulting binding energy differences were derived from the frequency dependence of the corresponding Al2p, Ce3d and O1s peaks. At low ceria loadings the main constituent on the surface is $CeAlO_3$ phase, while for high ceria loading the film is constructed from CeO_2 and $CeAlO_3$ phases spread over the Al_2O_3. Accordingly, it was observed that the ceria loading determines the conductivities of the investigated thin oxide films.

1. Introduction

Ceria (CeO_2) as one representative of rare-earth materials has focused attention of the scientist due to its unique properties which make it suitable for various applications such as catalysis and fuel cells [1,2]. Ceria's importance stems from its oxygen storage capability (OSC). The oxygen storage-and-release ability of ceria is a remarkable example of an electron quantum process directly manifesting itself in a macroscopic property used in many modern environmentally friendly applications. By releasing and storing oxygen during fuel-rich and fuel-lean conditions, the optimal oxygen pressure for the catalytic removal of harmful exhaust gases can be maintained. This is due to the partial reduction or oxidation of cerium and is related to the chemistry of oxygen vacancies in the material. Understanding of the effects of oxygen vacancy formation is crucial for a complete description of the mechanisms involved in the partial reduction/oxidation connected with the OSC of ceria.

Adding CeO_2 to Alpha-alumina improves its textural stability at high temperatures. The high thermal stability and the high reducibility of CeO_2/Al_2O_3 oxides [3] make them very attractive carriers for catalysts.

Wide varieties of physical and chemical processes have been developed for obtaining the CeO_2 as thin films with desirable properties; laser ablation [4], spray pyrolysis [5], magnetron sputtering [6], electrochemical deposition [7], and others. Preparation of ceria-containing catalytic materials with sufficiently high specific surface area is still not a well-developed technology. For these reasons, researches have focused their attention on the stabilization of dispersed cerium oxide on high surface area systems such as alumina. The electrochemical deposition could be one of the promising methods for preparation of ceria containing materials because of its advantage of low processing temperature, normal handling pressure, high purity of deposition, and controlled thickness of the film [7].

In particular for catalytic application the physicochemical properties and catalytic activities of the solid samples containing several oxides are generally different from that of the individual oxides alone, because of the fact that the activity of the "mixed oxides" could be the result of various interactions.

According to the electronic theory of catalysis, the rate and activation energy of reaction depend upon the Fermi level of the catalyst, and thus it can be expected that electronic interaction between metal oxides or metal and the support can extensively modify the Fermi level of the catalyst. Therefore, this interaction can influence the catalytic activity of sample. Accordingly, a parallelism was established between the changes in the electrical conductivity and in the catalytic activity [8]. The physical origin of this may be due to the fact that the electrical conductivity is determined by the free carrier concentration in the semiconductor on the one side; these take part in the catalytic reaction and determine its rate. The introduction of impurities (of a given nature or a given concentration) into the surface or in the bulk of the semiconductor is a factor which changes its electrical conductivity. Furthermore, both electrical and catalytic properties are highly affected by defects as well. In the particular case of the ceria, it is well established that the presence of Ce^{3+} states are unavoidable on the surface, which significantly contributes to both properties.

* Corresponding author at: Institute of General and Inorganic Chemistry, Bulgarian Academy of Sciences, Sofia 1113, Bulgaria. Tel.: +359 2 979 25 64.
E-mail address: iva@svr.igic.bas.bg (I. Avramova).

0040-6090/$ – see front matter © 2013 Elsevier B.V. All rights reserved.
http://dx.doi.org/10.1016/j.tsf.2013.03.049

X-ray photoelectron spectroscopy (XPS) as a surface sensitive method is also very useful for distinguishing between the Ce^{3+} and Ce^{4+} states in a mixed CeO_x oxide system. In addition, by employing it in a Dynamic mode, it is also possible to probe certain electrical properties of the materials under investigation. Recently Suzer et al. reported this method [9–13]. During the Dynamic mode, the sample is subjected to electrical impulses of various frequencies, and XPS is used to record the response of the system extracted from the measured charging shifts and broadening of the corresponding peaks. While conducting sample/domain/surface structure responded promptly and exhibits no frequency dependence to the impulses, a poorly conducting system responses very nonlinearly both in terms of the positions of the peaks and their frequency dependence. Therefore, the main aim of the present work is to investigate the CeO_x/Al_2O_3 thin films depending of cerium amount using XPS in a Dynamical mode with a hope to correlate the extracted electrical properties with their chemical and catalytic activities. Additional Scanning Electron Microscopy (SEM) characterizations of the system have been done, too.

2. Experimental part

The oxide films of alumina and ceria were consequently deposited electrochemically from nonaqueous electrolytes. The deposition of the alumina films proceeded in a working electrolyte consisting of saturated solution of absolute alcohol and 0.1 M $AlCl_3 \times 6H_2O$ salt. The cathodic deposition was performed in a potentiostatic regime at 5 V forming voltage. The deposition time was 60 min. The cathode substrate used was a stainless steel OC 404 (20.0% Cr, 5.0% Al, 0.02% C, and balance Fe). Platinated titanium mesh was used as counter electrode (anode). It was situated symmetrically around the working cathode and its surface was chosen specially to ensure a low anode polarization, which hindered Cl^- oxidation. Because of the relatively low equivalent conductance of the working electrolyte ($\chi \sim 1.10^{-2}\ \Omega^{-1}\ cm^{-1}$), it warmed up during the electrolysis. For this reason, the electrochemical deposition of alumina was carried out in a specially constructed, thermostated electrochemical cell. The cell was kept at a constant temperature of 15–18 °C by a water-cooling circulation. After careful washing in absolute alcohol the alumina coated specimens were covered galvanostatically (in the identical electrochemical cell) with ceria layers in a solution of 0.3 M $CeCl_3 \times 7H_2O$ diluted with absolute alcohol. The investigated deposition time was 5 and 80 min. The current density was $i = 0.3\ mA/cm^2$ and the temperature of the electrolyte was kept constant equal to 25 °C.

During the electrolysis, the anodic and cathodic areas were separated by an ion-exchange membrane (selective to Cl^- ions) in order to prevent the participation of Ce^{4+} (formed on the base of oxidation reaction $Ce^{3+}\text{-}e^- = Ce^{4+}$) on the platinated titanium anode. Thus, only Ce^{3+} ions were allowed to participate in the reduction process. The obtained CeO_x/Al_2O_3 on stainless steel substrate coatings have 1 and 2 μm thicknesses, respectively and are characterized with very good adhesion, according adhering tests [14]. Then as deposited thin oxide films on steel substrate have been calcinated in air at 450 °C for 2 h.

XPS measurements were carried out using a Thermo Fisher K-Alpha electron spectrometer with Al Kα X-rays (monochromatic), with a flood gun used for charge neutralization under the base pressure 10^{-7} Pa. The samples were gently cleaned by sputtering with a low-energy (200 eV) Ar + ion gun for 30 s. The spectra were acquired using 0.05 eV binding Energy (BE) steps. The samples were electrically connected through the sample holder, which is grounded or subjected to external ±10 V square wave pulses in the range 10^{-3} to 100 kHz, during recording of the O1s, Al2p and Ce3d X-ray photoelectron lines. The detailed information concerning the experimental set-up can be found elsewhere [9–13]. The photoelectron spectra were quantified using the peak area and Scofield's photo-ionization cross-sections. The peak fitting was performed by XPSPEAK4.1 software. The lineshape used to represent the O1s, Al2p and Ce3d peaks was a Gaussian–Lorentzian product function. The Ce3d multiplets correspond to the spin-orbital split $3d_{5/2}$ and $3d_{3/2}$ core holes was kept equal to 18.5 eV. Shirley and Tougaard background subtraction method was used for the samples with high and low ceria loadings, respectively during the fitting procedure.

The microstructure and morphology of the electrodeposited thin oxides films were carried out with a JEOL JSM 6390 (Japan) Scanning Electron Microscope (SEM), equipped with an ultrahigh resolution scanning system in a regime of secondary electron image (SEI). The used operation voltage was 20 kV.

3. Results

The XPS analysis is a well accepted technique for distinguishing the chemical states of the surface structures of the investigated materials. Surface charging could arise during the XPS measurement as a result of the photoelectron emission from non conductive samples. In most of the investigations the developed surface charging is compensated by the directed flow of low energy electrons and/or ions from a flood gun [15]. The surface charging can also be used to obtain useful information concerning the properties of the investigated materials, as reported by several groups [16–26]. Suzer and co-workers adopted a different strategy by application of a small (10 V) bias which, also allows controlling the surface charging of the system under investigation. Numerous applications using the voltage stress in d.c. or a.c. forms have been presented in detail [9–13].

Applying a voltage bias to the sample during XPS measurements leads to a shift in the position(s) of the photoelectron lines. For example, when ±10 V is applied to a conductive sample in the d.c. mode, the induced shifts are exactly 10.0 eV up and down the energy scale, with a difference of 20.0 eV. For nonconductive samples the measured values are always smaller.

The normal XPS spectra of the samples having different deposited cerium amount, recorded when the samples are grounded, are shown in Fig. 1 and the XPS data are summarized in the Table 1. As one can see from the figure the O1s peak for the sample having high ceria loading has a shoulder at higher binding energy next to the main peak situated at 529.7 eV, which is a typical value for the lattice oxygen in CeO_2 [27]. The higher binding energy feature at around 531.8 eV suggest the presence of Ce^{3+} related surface defects where oxygen occupies additional lattice sites like vacancy or oxide ions in a defective CeO_x ($x < 2$) [28] or formation of hydroxyl groups on the surface, or oxygen chemisorbed on the surface in other forms such as CO, CO_2 [29,30] and small contribution of oxygen which belongs to Al_2O_3 [31] exist, too. The O1s spectrum for low ceria loading has a single peak at around 532.0 eV, which Binding Energy slightly differs from that of electrodeposited Al_2O_3 on SS substrate at 531.4 eV [31].

The Al2p for both samples appears as single peak at a binding energy typical for Al in the oxide state. With increasing of deposited cerium amount, the maximum of the Al2p peak shifts to lower binding energy, which is accompanied by the decrease of its intensity [7]. The Ce3d spectra are rather complex since the peak is spin–orbit split into a doublet, with each doublet showing extra structures due to final state effects [29,30,32]. The principal labels, u and v, correspond to spin orbit pairs split while the superscripts denote a common final state occupation. Up to ten peaks can be distinguished in the spectra for the sample having high ceria loading. They arise from both oxidation states of cerium present in the electrodeposited oxide films, i.e. Ce^{3+} and Ce^{4+} respectively. The doublets labeled as v^{III} and u^{III} are unique to CeO_2 and result from a $Ce3d^9O2p^6Ce4f^0$ final state. An additional doublet referred to $3d_{3/2}$ and $3d_{5/2}$, also appears in the spectrum due to the presence of Ce_2O_3 (Ce in oxidation state (III)) and is assigned to v^I and u^I, respectively. The v^{III} and u^{III} as well as v^I and u^I are the best distinguished characteristic peaks to

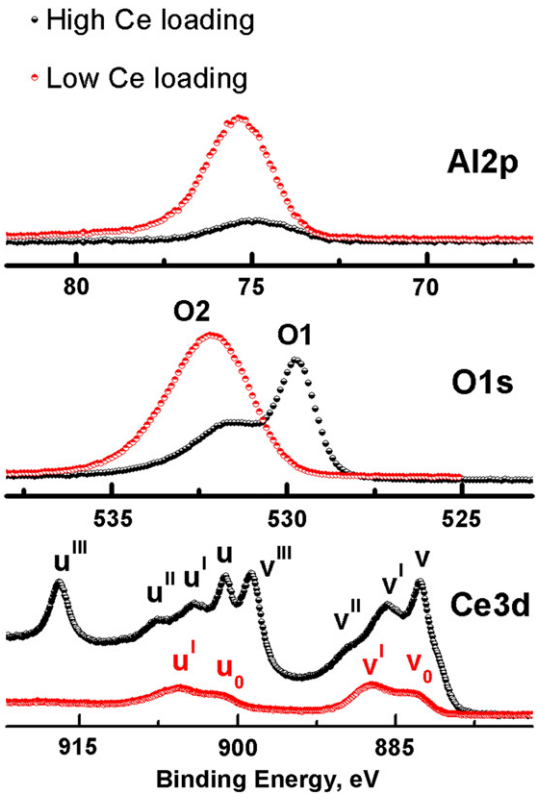

Fig. 1. The Al2p, O1s and Ce3d spectra for CeO_x/Al_2O_3 films on stainless steel with high and low ceria loading.

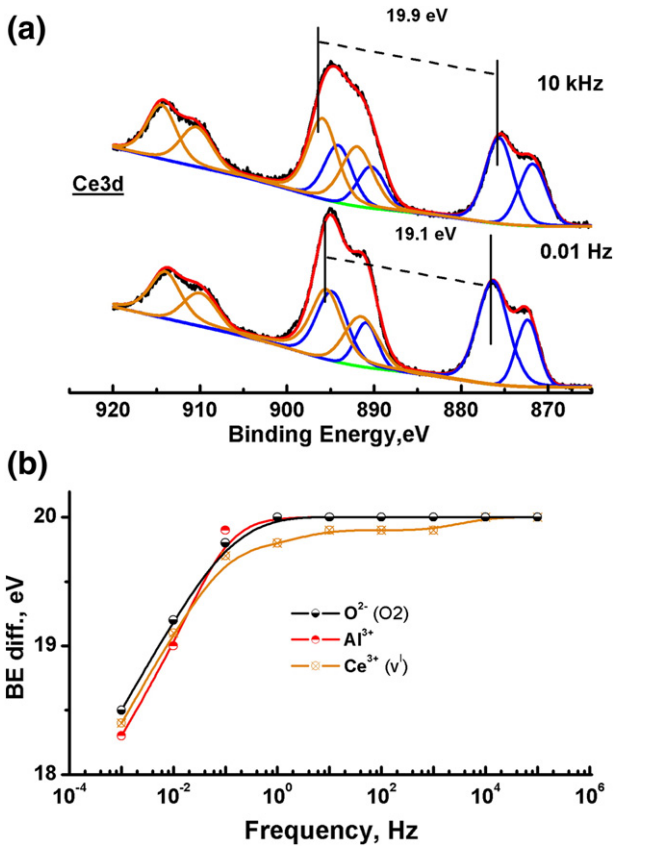

Fig. 2. (a) Ce3d spectra of CeO_x/Al_2O_3 on stainless steel-low ceria loading film recorded under ±10 V SQW excitation at low (0.01 Hz) and high (10 kHz) frequency regions. (b) The measured binding energy difference between the twinned Ce3d, O1s and Al2p peaks, plotted against the logarithm of the frequency.

differentiate Ce^{4+} from Ce^{3+}. The Ce3d line for the low ceria loading sample has only four peaks because the Ce $4f^0$ final state component lacks. The spectrum is typical for Ce_2O_3 oxide.

Next, dynamical measurements were carried out in order to extract more information about chemical composition as well as the electrical properties of these two samples. XPS measurements in the dynamic mode are performed, when the bias is introduced in the form of square waves with different frequencies. As a result, oxygen, aluminium and cerium photoelectron peaks for the sample having 1.8 at.% cerium on the surface are all twinned and the resulting BE differences are evaluated. The binding energy differences in the low frequency region are significantly smaller than 20.0 eV, while at high frequency part they become independent of frequency changes and reach the 20.0 eV value as shown in Fig. 2(a) and (b). Because of the complex Ce3d peak structure, due to the overlapping of the peaks as a result of applied voltages, for the observed changes we get information for the binding energy difference after careful deconvolution of the recorded Ce3d photoelectron lines at each frequency. The very important outcome of this analysis is the finding that the Al2p, O1s and Ce3d peaks all track each other as the frequency is varied, indicating a strong possibility that the $Ce_xAl_{2-x}O_3$ phase is the main constituent of the surface. The probable explanation of this, especially for low ceria loadings, is incorporation of Ce^{3+} cations into the vacant lattice octahedral sites in the Al_2O_3 lattice, resulting in a formation of $CeAlO_3$ precursor. This finding is consistent with the literature, where they show that the chemical state of cerium depends strongly on the ceria concentration in CeO_2/Al_2O_3 catalysts [33,34]. Similarly, Mauch and co-authors concluded that the Ce^{3+} spectral features increased with decreasing of CeO_2 content, and this was attributed to the formation of $CeAlO_3$ [35].

However, the dynamical response of the Al2p, O1s and Ce3d peaks for the sample having 20.4 at.% cerium on the surface is very different as presented in Fig. 3 (a) and (b). In this case, as was mentioned above the O1s peak has a shoulder at higher binding energy side, acting in response of frequency as well as the main peak. At low frequency region the higher energetic shoulder in O1s peak splits into two components, one exhibiting shifts around 3 eV, while for the other one the evaluated binding energy difference at low frequency region is 19.7 eV. For the main O1s peak the 19.6 eV difference was observed. The Al2p peak at low frequency exhibits strong charging shifts up to 3 eV, while at higher frequency it becomes independent. Again, by utilizing careful fitting procedure, we were able to separate the behaviour of the Ce^{3+} from that of the Ce^{4+} states using their respective responses during the frequency span. The Ce^{3+} and Ce^{4+} respond similarly as frequency changes. At low frequency we evaluate 19.8 eV and 19.6 eV differences for Ce^{3+} and Ce^{4+} states, respectively and 20.0 eV for both states at high frequency. As was evaluated previously, the frequency dependence of the difference in the binding energy between the left (+cycle) and the right (−cycle) peaks varies like an S-type curve, as well as the variations in the broadening of the peaks and this behaviour is material specific [11]. The results now confirm that this behaviour is also oxidation state specific for the ceria moieties. Accordingly, we state that, in this case, our system is mixed and consists of CeO_2 and $CeAlO_3$ moieties spread over alumina.

Table 1
Summary of XPS data for CeO_x/Al_2O_3 oxide films on stainless steel.

Sample	Oxygen		Aluminium		Cerium	
	BE(O1s), eV	at.%	BE(Al2p), eV	at.%	BE(Ce3d), eV	at.%
Low ceria loading	532.0	54	75.3	44.2	883.0	1.8
High ceria loading	529.7 531.8	66	74.9	13.6	882.6	20.4

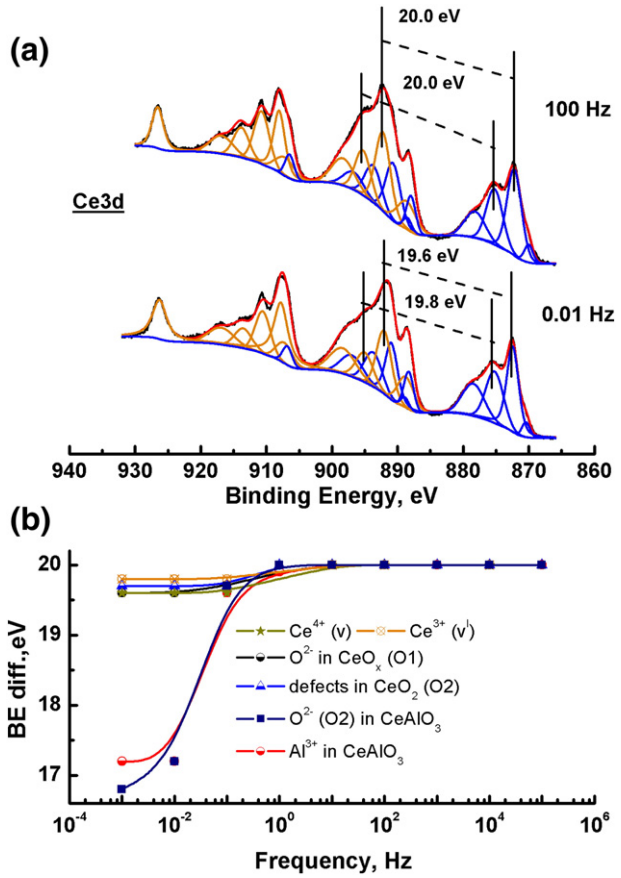

Fig. 3. (a) Ce3d spectra of CeO_x/Al_2O_3 on stainless steel-high ceria loading film recorded under ±10 V SQW excitation at low (0.01 Hz) and high (100 Hz) frequency regions. (b) The measured binding energy difference between the twinned Ce3d, O1s and Al2p peaks, plotted against the logarithm of the frequency.

A similar conclusion that CeO_2 coexists with $CeAlO_3$ precursor dispersed on the Al_2O_3 oxide was observed previously [36].

The morphology of CeO_x/Al_2O_3 samples which are a subject of the present study is shown in Figs. 4 and 5. The structure of the sample with low ceria loading is close to that for the pure Al_2O_3 films electrodeposited on stainless steel [31], additionally the small bright snail-like areas that belong to ceria are visible. An essential difference

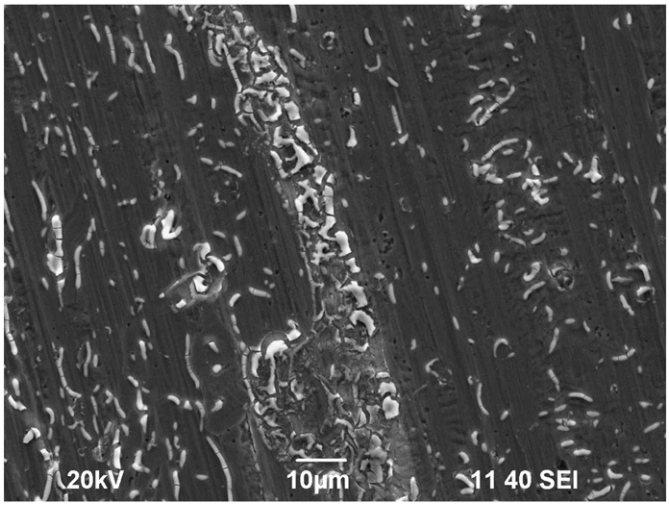

Fig. 4. SEM micrograph of low ceria loading CeO_x/Al_2O_3 oxide film electrodeposited on stainless steel substrate.

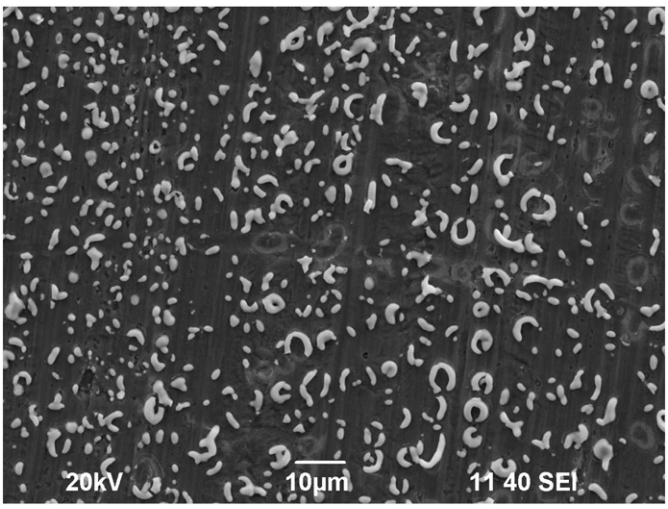

Fig. 5. SEM micrographs of high ceria loading CeO_x/Al_2O_3 oxide film electrodeposited on stainless steel substrate.

appears for the sample having high ceria loading. In this case the surface of the sample is almost uniformly covered by small bright snail-like areas of ceria on top of the Al_2O_3 support.

4. Discussion

XPS studies of core-level photoemission can provide information about the electronic character of mixed compounds. The chemical mixing of several types of metal and/or metalloid oxides to create a composite oxide is obviously a complex process. According to the above presented results taken in a normal and dynamical XPS mode the nature of the investigated system depends of cerium deposited amount on the surface.

When the samples are subjected to external a.c. stress, the position of the peaks shifts to lower or higher binding energy, respectively. It is well known that charge accumulation in oxide layers could be due to a various trapping mechanisms. However homogeneity of samples could play a crucial role in charge distribution and should be taken into account. In non homogeneous samples build-up of charge is a complicated process, because size, type and distribution of inhomogeneity all take part in charge build up [37].

In Ref. [38] the authors reported that thin Al-rich Al_2O_3 films exhibit the capability of both negative and positive charge trapping. It was observed that the charge trapping depends on the polarity of the applied voltage. The negative voltage caused the hole (absence of electron) trapping, while the positive voltage led to electron trapping. As conduction in the film could be enhanced by the hole trapping and reduced by the electron trapping. Ceria is an example of a mixed electron-ionic conductor. The electronic defect (e^-) can be regarded equivalent to the presence of Ce^{3+} ion. These electronic defects are accompanied by formation of ionic defects which in this case are oxygen vacancies. The concentration of oxygen vacancies is related to the deviation from stoichiometry "x" in CeO_{2-x} oxide. The electron conductivity of CeO_2 is attributed to small polaron hopping with thermally activated electron mobility [39]. In this case electron is self trapped at a given lattice site (Ce^{3+}) and can move only to an adjacent site by an activated hopping process. The greater is the deviation from the stoichiometry, the more evident the electronic contribution becomes.

Comparing the evaluated BE differences versus frequency for both CeO_x/Al_2O_3 on SS samples one can see the remarkable disparity of the frequency dependences of the Al^{3+}, Ce^{3+}, Ce^{4+}, O^{2-}, and oxygen belonged to defects states in CeO_2 lattice (see Figs. 2b and 3b). The frequency response of ionic states seems to depend on the host

oxide matrix. As can be seen the dependences of BE difference versus frequency for Al^{3+} in both samples have different behaviour. Since the Ce penetration in the Al_2O_3 host matrix is limited, nevertheless ceria and alumina could be mixed and form Ce-aluminate [40]. In our case in early 5 min deposition time of ceria cerium aluminate of Ce^{3+} electronic structure is grown. Forward increase of the deposition time of ceria will form sufficiently thick cerium aluminate layer that will block the diffusion of Al atom towards the interface and as a consequence pure ceria start to grow. So the probable explanation of different behaviour of Al^{3+} associated with cerium aluminate formation for both samples against BE difference could be its different stoichiometry.

Another interesting outcome can be done if one tries to compare the Ce^{3+} state frequency dependences. In case of low ceria loadings, Ce^{3+} follows the Al^{3+} response with a small delay at higher frequencies (see Fig. 2b), which is in agreement with above made proposal of existence of $CeAlO_3$ oxide, which prevents Ce^{3+}/Ce^{4+} cycling [41]. The evaluated BE difference in low frequency region is around 3 eV lower than 20 eV and reach 20 eV at higher frequencies, which is the evidence that the formed film is poorly conductive.

When the cerium amount on the surface increase, which is obvious from XPS as well as from SEM results we can suppose that the host matrix is CeO_2. In this case the frequency response of Ce^{4+} and Ce^{3+} surface states is remarkably different in comparison to Al^{3+} states frequency response (see Fig. 3b). It is well known that once Ce^{3+} appears in CeO_2 lattice, oxygen vacancy will be generated to maintain electrostatic balance according to the following equation [42]:

$$4Ce^{4+} + O^{2-} -> 4Ce^{4+} + 2e^{-}/\square + 1/2O_2 -> 2Ce^{4+} + 2Ce^{3+} + 1/2O_2 + \square$$

In the above equation the "□" represents an empty position (anion-vacant site) that originating from the removal of O^{2-} from the CeO_2 lattice. Thus, upon oxygen vacancy formation in CeO_2, two electrons are left behind, and they localize on the f-level traps of two of the neighboring Ce atoms, turning their formal valence from Ce^{4+} to Ce^{3+}.

The frequency responses of Ce^{4+} and O^{2-} states are equal; because the evaluated BE difference at low frequency is 19.6 eV. One can see that Ce^{3+} and oxygen states associate with defects in the CeO_2, or OH^- groups have approximately same character but with a small delay from each other, 19.8 eV and 19.7 eV respectively. This could be linked with the existence of Ce^{3+} — vacancy associates. In other words, the formation of reduced cerium oxides is a formation, migration, and ordering of Ce^{3+}-vacancy complexes, which confirm earlier results [43].

Haneda et al. [44] have reported that CeO_2, CeO_{2-x}/Al_2O_3 and $CeAlO_3/Al_2O_3$ showed a decrease in OSC value in the order CeO_{2-x} > $CeAlO_3$ > small sized CeO_2 > large CeO_2 crystallites.

Accordingly playing with the deviation from the stoichiometry in CeO_{2-x} oxide and in the present case with deposited cerium amount one can rule the conductivity of the film as well as it reducibility.

5. Conclusions

In summary in the above presented study we introduce the application of dynamic X-ray photoelectron spectroscopy method as a powerful tool for studying the oxidation states behaviour of CeO_x/Al_2O_3 on stainless steel substrate systems applied in catalysis. The main constituent on the surface is $CeAlO_3$ phase for low ceria loading sample, while for high ceria loading the film is constructed from CeO_2 and $CeAlO_3$ phases spread over the Al_2O_3. We showed that the film conductivity could be ruled by ceria loading. The conductivity increases with increasing cerium deposited amount. We found out that the Ce^{3+} states frequency response depends of host oxide matrix.

Acknowledgements

Research sustained by the European Union 7th Framework Project Unam-Regpot (Grant No. 203953) funds.

References

[1] A. Trovarelli, Catal. Rev. Sci. Eng. 38 (1996) 439.
[2] J.L.M. Rupp, T. Drobek, A. Rossi, L.J. Gauckler, Chem Mater. 19 (2007) 1134.
[3] S. Damyanova, C.A. Perez, M. Schmal, J.M.C. Bueno, Appl. Catal. Gen. 234 (2002) 271.
[4] T. Chaudhuri, S. Phok, R. Bhattacharya, Thin Solid Films 515 (2007) 6971.
[5] B. Elidrissi, M. Addou, M. Regragui, C. Monty, A. Bougrine, A. Kachouane, Thin Solid Films 379 (2000) 23.
[6] M.T. Ta, D. Briand, Y. Guhel, J. Bernard, J.C. Pesant, B. Boudart, Thin Solid Films 517 (2008) 450.
[7] P. Stefanov, G. Atanasova, D. Stoychev, Ts. Marinova, Surf. Coat. Technol. 180 (2004) 446.
[8] D.D. Eley, in: D.D. Eley, P.W. Selwood, Paul B. Weisz (Eds.), Advanced in Catalysis, vol. 12, Academic Press, New York and London, 1960.
[9] S. Suzer, A. Dana, J. Phys. Chem. B 110 (2006) 19112.
[10] H. Sezen, G. Ertas, A. Dana, S. Suzer, Macromolecules 40 (2007) 4109.
[11] S. Suzer, H. Sezen, A. Dana, Anal. Chem. 80 (2008) 3931.
[12] H. Sezen, G. Ertas, S. Suzer, J. Electron Spectrosc. Relat. Phenom. 178 (2010) 373.
[13] S. Suzer, H. Sezen, G. Ertas, A. Dana, J. Electron Spectrosc. Relat. Phenom. 176 (2010) 52.
[14] Review of Methods Available for Testing Adhesion of Electrodeposited and Chemically deposited Metallic Coatings on Metallic Substrates, BS 5411: Part 10; 1981/ISO 2819, 1980.
[15] T.L. Barr, J. Vac. Sci. Technol. A 7 (1989) 1677.
[16] W.M. Lau, X.W. Wu, Surf. Sci. 245 (1991) 345.
[17] D.F. Mitchell, K.B. Clark, J.A. Bardwell, W.N. Lennard, G.R. Massoumi, I.V. Mitchell, Surf. Interface Anal. 21 (1994) 44.
[18] B.J. Tielsch, J.E. Fulghum, Surf. Interface Anal. 24 (1996) 422.
[19] B.J. Tielsch, J.E. Fulghum, D.J. Surnam, Surf. Interface Anal. 24 (1996) 459.
[20] B.J. Tielsch, J.E. Fulghum, Surf. Interface Anal. 25 (1997) 904.
[21] J. Cazaux, J. Electron Spectrosc. Relat. Phenom. 113 (2000) 15.
[22] I. Doron-Mor, A. Hatzor, A. Vaskevich, T. van der Boom-Moav, A. Shanzer, I. Rubinstein, S.R. Cohen, H. Cohen, Nature 406 (2000) 382.
[23] K. Shabtai, I. Rubinstein, S.R. Cohen, H. Cohen, J. Am. Chem. Soc. 122 (2000) 4959.
[24] M. Dubey, I. Gouzman, S.L. Bernasek, J. Schwartz, Langmuir 22 (2006) 4649.
[25] A. Islam, M. Mukherjee, J. Phys. Chem. B 112 (2008) 8523.
[26] A. Rozenblat, Y. Rosenwaks, L. Segev, H. Cohen, Appl. Phys. Lett. 94 (2009) 053116.
[27] M. Romeo, K. Bak, J. El Fallah, F. Normand, L. Hilaire Le, Surf. Interface Anal. 20 (1993) 508.
[28] A. Pfau, K.D. Schierbaum, Surf. Sci. 321 (1994) 71.
[29] D.R. Mullins, S.H. Overbury, D.R. Huntley, Surf. Sci. 409 (1998) 307.
[30] K. Schierbaum, Surf. Sci. 399 (1998) 29.
[31] D. Stoychev, P. Stefanov, D. Nikolova, A. Aleksandrova, G. Atanasova, Ts. Marinova, Surf. Coat. Technol. 180–181 (2004) 441.
[32] M.V. Rama Rao, T. Shripathi, J. Electron Spectrosc. Relat. Phenom. 87 (1997) 121.
[33] J.Z. Shyu, W.H. Weber, H.S. Gandhi, J. Phys. Chem. 92 (1988) 4964.
[34] K. Bak, L. Hilaire, Appl. Surf. Sci. 70–71 (1993) 191.
[35] R.H. Mauch, K.O. Velthaus, G. Bilger, H.W. Schock, J. Cryst. Growth 117 (1992) 964.
[36] I. Avramova, P. Stefanov, D. Nicolova, D. Stoychev, Ts. Marinova, Comput. Sci. Technol. 65 (2005) 1663.
[37] D.R. Baer, M.H. Engelhard, D.J. Gaspar, A.S. Lea, C.F. Windisch Jr., Surf. Interface Anal. 33 (2002) 781.
[38] Y. Liu, T.P. Chen, W. Zhu, M. Yang, Z.H. Cen, J.I. Wong, Y.B. Li, S. Zhang, X.B. Chen, S. Fung, Appl. Phys. Lett. 93 (2008) 142106.
[39] H. Tuller, A. Nowick, J. Phys. Chem. Solids 28 (1977) 859.
[40] R. Sohal, G. Lupina, O. Seifarth, P. Zaumseil, Ch. Walczyk, Th. Schroeder, Surf. Sci. 604 (2010) 276.
[41] G. Zhou, P.R. Shah, T. Montini, P. Fornasiero, R.J. Gorte, Surf. Sci. 601 (2007) 2512.
[42] A. Trovarelli, in: A. Trovarelli (Ed.), Catalytic Science Series, vol. 2, Imperial College Press, London, 2002, p. 15.
[43] N.V. Skorodumova, S.I. Simak, B.I. Lundqvist, I.A. Abrikosov, B. Johansson, Phys. Rev. Lett. 89 (2002) 166601.
[44] M. Haneda, T. Mizushima, N. Kakuta, A. Ueno, Y. Sato, S. Matsuura, K. Kasahara, M. Sato, Bull. Chem. Soc. Jpn. 66 (1993) 1279.